Eur. Phys. J. Plus (2024) 139:312
https://doi.org/10.1140/epjp/s13360-024-05088-0

THE EUROPEAN PHYSICAL JOURNAL PLUS

Review

Dynamics of molecules in torsional DNA exposed to microwave and possible impact on its deformation: stability analysis

M. Tantawy[1,a], **H. I. Abdel-Gawad**[2]

[1] Department of Basic Sciences, Faculty of Engineering, October 6 University, Giza, Egypt
[2] Department of Mathematics, Faculty of Science, Cairo University, Giza, Egypt

Received: 25 November 2023 / Accepted: 11 March 2024
© The Author(s) 2024

Abstract In this work, we explore the dynamics of molecules in torsionally stressed DNA subjected to periodic external forces, specifically microwave radiation. Our approach involves constructing a novel continuum model based on a discrete model. Remarkably, this continuum model has not been analytically solved in existing literature, which motivates us to derive analytic solutions for investigating DNA s dynamical behavior. Our primary objective is to examine the impact of an external field (such as microwave radiation) on DNA dynamics, potentially affecting its structural integrity. Scientifically, we know that DNA molecules exposed to microwaves can suffer damage. Here, we focus on stability (or instability) to determine deterministic outcomes. Analytic solutions are essential for this purpose. The model equations governing torsional DNA (TDNA) behavior are non-autonomous and, in some cases, not integrable, meaning no exact solutions exist. Consequently, we rely on approximate solutions. Our chosen method is the extended unified method, allowing us to control errors through parameter selection. We consider two scenarios: when the torsional angle is smaller than one or completely free. Exact solutions emerge only when stacking and chain curvature constants are equal, otherwise, we derive approximate solutions. Numerical results: Numerical representations reveal that the localization of DNA molecules depends significantly on the microwave amplitude (MWA) and damping rate. Additionally, a critical MWA or DA value exists beyond which TDNA undergoes deformation. Stability analysis plays a crucial role in understanding these intricate dynamics. The present study sheds light on the interplay between external fields, DNA stability, and structural changes. Analytic solutions provide valuable insights into this complex system, with potential implications for biological processes and health.

1 Introduction

The dynamics of DNA in the absence of an external force were currently studied in the literature's. Researchers have investigated the behavior of DNA molecules when confined within pores. Specifically, they measured the escape time for DNA molecules initially drawn into these tiny spaces. This research provides insights into how DNA responds in confined environments [1]. The dynamics of DNA molecules in mixed flows, where the ratio of vorticity to strain rate plays a crucial role, have been examined using Brownian dynamics simulations. Understanding how DNA behaves under varying fluid flow conditions is essential for biological processes [2]. Scientists have used optical tweezers to probe the elastic response of single plasmoid and lambda phage DNA molecules. These experiments provide valuable information about DNA's mechanical properties, especially when subjected to trivalent cations [3]. While, in [4], The dynamics of isolated DNA molecules under homogeneous extensional flow have been reported. Browning dynamics simulations have been employed to study a single DNA molecule's behavior in shear flow with internal viscosity. Investigating how DNA moves and deforms under shear forces contributes to our understanding of its dynamics [5].

The Peyrard–Bishop (PB) DNA model was used to study the dynamical properties of double-stranded DNA using Langevin dynamics [1–3]. The PB model is a one-dimensional coarse-grained lattice model at the base pair level, considering a continuous variable at each site which describes the stretching of individual base pairs [4]. The mechanical stability and elasticity properties of duplex DNA molecules were studied numerically within the frame of a network model with the arrangement of the base pairs. A discrete worm-like chain model and Brownian dynamics were used to simulate the DNA/RNA buckling transition [5–8]. The worm-like chain (WLC) model in polymer physics is used to describe the behavior of polymers that are semi-flexible [5]. The fluctuational dynamics of a tagged base pair in double-stranded DNA was studied [9–12]. This involves the disruption of hydrogen bonds between the complementary bases and flipping the base out of the helical stack disrupting two contacts [11]. The dynamics of a double-stranded DNA (dsDNA) segment, as a semi-flexible polymer, in a shear flow, was studied [1, 3, 11, 12]. In physics, Brownian dynamics is a mathematical approach for describing the dynamics of molecular systems in the diffusive regime [16].

[a] e-mail: mtantawymath@gmail.com (corresponding author)

Published online: 05 April 2024

These studies provide valuable insights into the complex dynamics and properties of DNA, contributing to our understanding of its function in biological systems.

The effects of helicity and inhomogeneities, which are due to the site-dependent stacking and hydrogen bonding energies in DNA and protein molecules, on DNA base pairs opening were investigated numerically [13].

The dynamics state damage DNA or DNA at a defect were studied in biochemistry, physical chemistry, medicine and in biology [14–18]. The study of dynamics of DNA, in this state, had received the attention of many works. To this issue, a discrete model to describe the nonlinear dynamics DNA molecule with inharmonic potential, which imposes inhomogeneity, were studied in [19].

The dynamics of DNA are investigated mathematically via discrete and continuum models, where solutions of these models have attired the attention of many research works. In this context, the double-chain model for DNA was studied analytically to extract the traveling wave solutions [2, 20–23]. Solution of the minimum-energy shape of circular DNA, showing that twist-bend coupling induces sinusoidal twist waves was performed [24]. Diverse performances for the solitary wave solutions to the DNA PB Model with Beta-Derivative via three distinctive techniques were investigated [25].

In [26], DNA-torsional model was reduced to the sine-Gordon and double sine-Gordon equations with Caputo fractional was used. The dynamics of DNA in the presence of an external force were currently studied. the molecular dynamics of DNA under the influence of external periodic force were investigated within the framework of a mechanical model without simplifications [27]. In [28], the impact of the damping effect and external forces on DNA breathing was investigated. The dynamics of DNA in the presence of uniform damping and periodic force was studied [29].

The most relevant works to the present study were carried in [30–33]. It is worth mentioning that, some of these works studied torsional DNA in the absence of an external force, while others studied non-torsional DNA in the presence of an external force. So, no comparison with the present work is amenable.

The most eminent question is, how to be able to inspect the dynamic behavior and to study the impact on the DNA molecules structure?

Our objective, here, is to discuss the most acceptable answer.

Here, a continuum model for torsional DNA is considered, in the presence of an external force, which is taken, here, a microwave. It is derived based on a discrete model which was proposed in [34]. Exact and approximate solutions of the model equations are derived by using the extended unified method (EUM) [35–37].

2 The model equations and the EUM

2.1 The discrete model

From Fig. 1, the bases will be described by two coordinates P_n, P_n', and the rotation angle between next neighbor of bases φ_n and φ_n', referring to site $n \in N$on the two chain [31, 32].

A discrete model for torsional DNA under the influence of periodic external force was presented [33],

The Lagrange function and equations are

$$L = T - V, \tag{1}$$

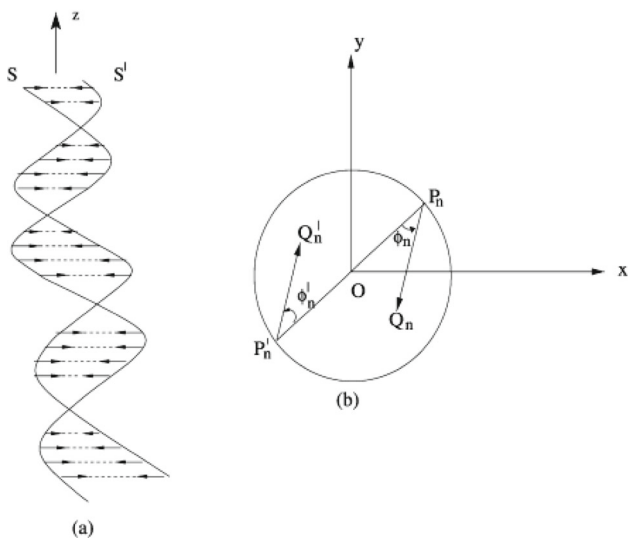

Fig. 1 Show rotational DNA molecules

where T and V are kinetic and potential energies,

$$T = \left[\sum_{n=1}^{N} \frac{m}{2}\left[(\dot{P}_n)^2 + (\dot{P'}_n)^2\right] + \frac{I}{2}\left[(\dot{\varphi}_n)^2 + (\dot{\varphi'}_n)^2\right],$$
$$V = V_1 + V_2. \tag{2}$$

The effect of stacking is,

$$V_1 = \frac{1}{2}\left[\sum_{n=1}^{N-1} \kappa_1\Big((P_{n+1} - P_n)^2 + \big(P'_{n+1} - P'_n\big)^2\Big)\, \kappa_2\Big((\varphi_{n+1} - \varphi_n)^2 + G_{02}\big(\varphi'_{n+1} - \varphi'_n\big)^2\Big) + \sum_{n=2}^{N} \text{terms}, n \to n-1\right], \tag{3}$$

and V_2 describes the coupling energy associated to the twist φ_n and φ'_n [34]

$$V_2 = \eta_1(n) \sum_{n=1}^{N-1} P_n\big(1 - \cos(\varphi_n - \varphi'_n)\big), \tag{4}$$

where m is center of mass, I the moment of inertia, κ_1, κ_2 are stacking and chain curvature constants, respectively. $\eta_1(n)$ indicate the site dependent character of H bonds between complementary DNA molecules.

For convenience, we write,

$$\varphi_n^{(\pm)} = \frac{\varphi_n \pm \varphi'_n}{2},\ P_n^{(\pm)} = \frac{P_n \pm P'_n}{2}. \tag{5}$$

In the case of the twist stretching, we have $P_n^{(+)} = -P_n^{(-)}$and $\varphi_n^{(+)} = -\varphi_n^{(-)}$ for simplicity we remove the sub and supper the superscripts. Here, we investigated the effect of various frequencies of external periodic action on the dynamics of a DNA molecule.

By using Eqs. (1)–(5), the discreet Lagrange equations are,

$$\begin{aligned} m\ddot{R}_n &= \kappa_1(R_{n+1} + R_{n-1} - 2R_n) - \eta(n)\,(1 - \cos\varphi_n), \\ I\ddot{\varphi}_n &= \kappa_2(\varphi_{n+1} + \varphi_{n-1} - 2\varphi_n) - \eta(n)\, R_n \sin\varphi_n + F(t), \end{aligned} \tag{6}$$

where$P_n = R_n$. The magnitude of the external influence is taken equal to $F(n, t) = -\beta\, \frac{\partial \varphi_n}{\partial t} + f\, \cos\varphi_n$ where the term $-\beta\, \frac{\partial \varphi_n}{\partial t}$ models the effects of dissipation caused by the interaction with the liquid surrounding the DNA molecule, and the term $f\, \cos\varphi_n$ models external periodic influence [34].

2.2 The continuum model

As continuum distribution in a plane, where the distance between two successive bases along the axis of the two chain ($\delta = 3.44A_0$) [24, 32].

$$\begin{aligned} R_n &= R(x,t), \varphi_n = \varphi(x,t), \\ R_{n\pm1} &= R(x,t) \pm \delta\, R_x(x,t) + \frac{1}{2}\delta^2 R_{xx}(x,t), \\ \varphi_{n\pm1} &= \varphi(x,t) \pm \delta\, \varphi_x(x,t) + \frac{1}{2}\delta^2 \varphi_{xx}(x,t), \end{aligned} \tag{7}$$

From Eq. (7) into Eq. (6) leads to,

$$\begin{aligned} &\frac{\partial^2 R(x,t)}{\partial\, t^2} - \kappa_1 \frac{\partial^2 R(x,t)}{\partial x^2} - \eta(1 - \cos(\varphi(x,t))) = 0, \\ &\frac{\partial^2 \varphi(x,t)}{\partial t^2} - G\frac{\partial^2 \varphi(x,t)}{\partial x^2} - \eta\, R(x,t)\sin(\varphi(x,t)) + \beta\frac{\partial \varphi(x,t)}{\partial t} - f\cos(\omega t) = 0. \end{aligned} \tag{8}$$

where R and φ stand for the distance between two bases and the torsional angle, respectively. In (8),

$\bar{\kappa}_1 = \frac{\kappa_1\delta^2}{m}$, $\bar{\kappa}_2 = \frac{\kappa_2\delta^2}{I}$ and for simplicity we omit upper bar ($\bar{\kappa}_1 = \kappa_1$, $\bar{\kappa}_2 = \kappa_2$) and $\eta = \frac{\eta_1(n)}{mI}$ takes two values $\eta_a$and η_b by their concentration, and $\eta = sN\, \eta_a - (1 - s\, \eta_b)$ (sN number of A- site of chain [33]).

To find the solutions of Eq. (8), we distinguish two cases:

(i) when $\varphi << 1$
(ii) φ is arbitrary.

In case (i), consider the two cases; (i_1) when $\cos(\varphi) \simeq 1 - \frac{\varphi^2}{2}$, $\sin(\varphi) \simeq \varphi$, ($i_2$) when $\cos(\varphi) \simeq 1 - \frac{\varphi^2}{2}$, $\sin(\varphi) \simeq \eta\, \varphi$-$\frac{\varphi^3}{3}$.

In case (ii), we use the transformation $\varphi(x,\, t) = \arctan(\frac{1}{2}(v(x,\, t) - \frac{1}{v(x,t)})$.

As Eq. (8) depends explicitly on t due to the presence of an external force, so, the similarity solutions are invoked. To this issue, we introduce the similarity transformations $R(x,\,t) = r(z,\,t),\ \varphi(x,\,t) = \theta(z,\,t)$, $z = h(t)\,x$, and $t = t$, and Eq. (3) becomes,

$$\begin{aligned}
&\frac{\partial^2 r(z,t)}{\partial\, t^2} - \kappa_1\, h(t)^2\, \frac{\partial^2 r(z,t)}{\partial z^2} - \eta\,(1 - \cos(\theta(z,t))) = 0,\\
&\frac{\partial^2 \varphi(x,t)}{\partial t^2} - \kappa_2\, h(t)^2\, \frac{\partial^2 \theta(z,t)}{\partial z^2} - \eta\, r(z,t)\sin(\theta(z,t)) + \beta\frac{\partial \theta(z,t)}{\partial t} - f\,\cos(\omega t) = 0.
\end{aligned} \tag{9}$$

Exact and approximate solutions of Eq. (9) are found by using the EUM, which asserts that the solutions of nonlinear evolution equations are expressed in polynomial and rational forms in an auxiliary function the satisfies appropriate auxiliary equations.

2.3 Brief account of the EUM

2.3.1 Polynomial solutions

For Eq. (9), these solutions are written,

$$\begin{aligned}
&r(z,t) = A(t)\sum_{i=0}^{n_1} a_i\phi(z,t)^i,\ \theta(z,t) = B(t)\sum_{i=0}^{n_2} b_i\phi(z,t)^i,\\
&\phi_z(z,t) = \lambda\sum_{i=0}^{k} c_i\phi(z,t)^i,\ \phi_t(z,t) = \mu(t)\sum_{i=0}^{k} c_i\phi(z,t)^i.
\end{aligned} \tag{10}$$

Here, the integrability of Eq. (9) is related to the existence of exact solutions of (10). In fact (10) holds if there exist integers n_1, $n_2$and k. To examine this, two conditions have to hold, the balance condition (BC) and the consistency condition (CC). This depends heuristically on the choice of the cases for $\theta(x,\,t)$ mentioned in the above. When taking, $\cos(\theta) \simeq 1 - \frac{\theta^2}{2}$, $\sin(\theta) \simeq \theta$, the BC reads $n_1 = n_2 = 2(k-1)$. For CC, we find that, the number of equations result, by setting the coefficients of $\phi(z,\,t)^j,\ j = 0,\,1,\,2,\,...etc$ equal to zero, is $(4k-3)$, and the number of parameters $\{a_j,\,c_j,\,b_j\}$is $(2k+1)$. The CC reads $4k - 3 - (2k+1) \le l$, where l is the highest order derivative ($l = 2$), so $1 \le k \le 3$.

It is worth mentioning that when Eq. (9) is integrable, the solutions of the equations that result from setting the coefficients of $\phi(z,\,t)^j,\ j = 0,\,1,\,2,\,$...etc equal to zero are consistent. If Eq. (9) is not integrable, in the sense that no exact solution exists, we are led to find approximate solutions. This is carried out by taking some coefficients of $\phi(z,\,t)^j,\ j = 0,\,1,\,2,\,$...etc are not identically zero. In this case, they are considered as errors in the solution (residue terms (RTs)).

As Eq. (9) depends explicitly on time, then similarity solutions are invoked. In this case, the errors are time dependent. The maximum error (ME) is controlled by an adequate choice of the values of the parameter in the RTs.

It is observed that the EUM, used here, is of lower time cost in symbolic computation when compared with the method of Lie symmetry as the later requires a hierarchy of long steps.

2.3.2 Rational solutions

The rational solutions of Eq. (9) are expressed in the form,

$$\begin{aligned}
&r(z,t) = A(t)\frac{a_1\phi(z,t) + a_0}{s_1\phi(z,t) + s_0},\ \theta(z,t) = B(t)\frac{b_1\phi(z,t) + b_0}{s_1\phi(z,t) + s_0},\\
&g_z(z,t) = \lambda\sum_{j=0}^{j=k} c_j\phi(z,t)^j,\ \phi_t(z,t) = \mu(t)\sum_{j=0}^{j=k} c_j\phi(z,t)^j.
\end{aligned} \tag{11}$$

A discussion similar to that given in Sect. 2.3.1 holds.

3 When $\varphi << 1$, $\cos(\varphi) \simeq 1 - \frac{\varphi^2}{2}$, $\sin(\varphi) \simeq \varphi$

In this case, Eq. (9) reduce to,

$$\begin{aligned}
&-\kappa_1\, h(t)^2\frac{\partial^2}{\partial x^2}r(z,t) + \frac{\partial^2}{\partial t^2}r(z,t) - \frac{1}{2}\eta\,\theta(z,t)^2 = 0,\\
&-\kappa_2\, h(t)^2\frac{\partial^2}{\partial x^2}\theta(z,t) - \eta\, r(z,t)\theta(z,t) + \beta\frac{\partial}{\partial t}\theta(z,t) + \frac{\partial^2}{\partial t^2}\theta(z,t) - f\,\cos(t\omega) = 0.
\end{aligned} \tag{12}$$

3.1 Polynomial (exact) solutions

When $k = 2$ and $n_1 = n_2 = 2$. in this case, the solutions of Eq. (12) are expressed by,

$$\begin{aligned} r(z,t) &= A(t)\big(a_2\phi(z,t)^2 + a_1\phi(z,t) + a_0\big),\\ \theta(z,t) &= B(t)\big(b_2\phi(z,t)^2 + b_1\phi(z,t) + b_0\big), \end{aligned} \tag{13}$$

and the auxiliary equations are,

$$\begin{aligned} \phi_z(z,t) &= \lambda\big(c_2\phi(z,t)^2 + c_1\phi(z,t) + c_0\big),\\ \phi_t(z,t) &= \mu(t)\big(c_2\phi(z,t)^2 + c_1\phi(z,t) + c_0\big). \end{aligned} \tag{14}$$

From Eqs. (13) and (14) and by setting the coefficients of $\phi(z,\ t)^j,\ j = 0,\ 1,\ 2,\ ...etc$ equal to zero leads to,

$$\begin{aligned} A(t) &= \frac{6c_2^2\big(\mu(t)^2 - \kappa_2\lambda^2 h(t)^2\big)}{a_2\eta},\ B(t) = \frac{6c_2^2\sqrt{2\kappa_1\lambda^2 h(t)^2 - 2\mu(t)^2}\sqrt{\kappa_2\lambda^2 h(t)^2 - \mu(t)^2}}{b_2\eta}, \kappa_2 = \kappa_1,\\ \mu''(t) &= \frac{1}{2a_2b_2^2\mu(t)}\big(\kappa_1^2\lambda^4 h(t)^4(a_2\big(-4b_2^2\big(c_1^2 + 2c_0c_2\big) + 12b_0b_2c_2^2 + 6b_1^2c_2^2\big)\\ &\quad - 3a_1b_2^2c_1c_2) - a_1b_2^2c_2\mu(t)^2\big(3c_1\mu(t)^2 + 5\mu'(t)\big) - 2a_2\big(-3b_1^2c_2^2\mu(t)^4\\ &\quad - 6b_0b_2c_2^2\mu(t)^4 + b_2^2\big(5c_1\mu(t)^2\mu'(t) + 2c_1^2\mu(t)^4 + 4c_0c_2\mu(t)^4 - \kappa_1\lambda^2 h'(t)^2\\ &\quad +\mu'(t)^2\big)\big) + \lambda^2 h(t)^2\kappa_1\big(a_1b_2^2c_2\big(6c_1\mu(t)^2 + \mu'(t)\big) + 2a_2\big(-6b_1^2c_2^2\mu(t)^2\\ &\quad - 12b_0b_2c_2^2\mu(t)^2 + b_2^2\big(c_1\mu'(t) + 4c_1^2\mu(t)^2 + 8c_0c_2\mu(t)^2\big)\big)\big)\\ &\quad +2b_2^2\kappa_1\lambda^2 h(t)\big(2a_1c_2\mu(t)h'(t) + a_2\big(4c_1\mu(t)h'(t) + h''(t)\big)\big)\big),\\ \mu'(t) &= \frac{1}{P}\big(\kappa_1^2\lambda^4 h(t)^4(a_1b_2c_2 + a_2(5b_2c_1 - 6b_1c_2)) - 2\lambda^2 h(t)^2(a_1b_2c_2\\ &\quad + a_2\big(5b_2c_1 - 6b_1c_2\big))\kappa_1\mu(t)^2 + \mu(t)^4(a_1b_2c_2 + a_2(5b_2c_1 - 6b_1c_2))\\ &\quad -4a_2b_2\kappa_1\lambda^2 h(t)\mu(t)h'(t)\big),\ P = a_2b_2\big(\kappa_1\lambda^2 h(t)^2 - 5\mu(t)^2\big),\\ b_1 &= \frac{2b_2c_1}{3c_2},\ a_0 = \frac{3\big(a_2^3\big(6b_0^2c_2^2 - 2b_2^2c_0^2\big) + a_1^2a_2b_2^2c_0c_2\big)}{b_2\big(2a_2^2\big(18b_0c_2^2 + b_2\big(c_1^2 - 12c_0c_2\big)\big) + 3a_1^2b_2c_2^2\big)},\\ b_0 &= \frac{5a_1^2b_2}{12a_2^2},\ c_1 = \frac{2a_1c_2}{a_2},\ \mu(t) = \frac{\sqrt{9a_2^2\beta^2 + 64a_1^2c_2^2\kappa_1\lambda^2 h(t)^2} - 3a_2\beta}{8a_1c_2},\\ h'(t) &= \frac{13401a_2\beta^2\left(\sqrt{9a_2^2\beta^2 + 64a_1^2c_2^2\kappa_1\lambda^2 h(t)^2} - 3a_2\beta\right)}{139776a_1^2c_2^2\kappa_1\lambda^2 h(t)} + \frac{h(t)^2}{a_1^2c_2^2\kappa_1\lambda^2}\\ &\quad \left(\frac{60992\sqrt{9a_2^2\beta^2 + 64a_1^2c_2^2\kappa_1\lambda^2 h(t)^2}}{a_2} - 325920\beta\right),\ c_0 = \frac{221a_1^2c_2}{252a_2^2}. \end{aligned} \tag{15}$$

In Eq. (15), equations for $\mu'(t)$ and $\mu''(t)$exist, so, the compatibility equation $(\mu'(t))'$-$\mu''(t) = 0$ is used, which gives rise to,

$$h(t) = \frac{\left(\sqrt{7}a_2\right)\sqrt{9\beta^2\sqrt{f}\sqrt{\eta}\sqrt{\cos(t\omega)} + 14\sqrt[4]{2}f\eta\cos(t\omega)}}{6\,2^{3/8}a_1\beta c_2\sqrt{\kappa_1}\lambda}. \tag{16}$$

By using Eqs. (13)–(16), the exact solution of (12) is,

$$\begin{aligned} R(x,t) &= \left(\frac{9a_2\beta^2 - a_2\left(9\beta^2 + 28\sqrt[4]{2}\sqrt{f}\sqrt{\eta}\sqrt{\cos(t\omega)}\right)}{17472a_1a_2c_2\eta}\right)\\ &\quad \left(78\sqrt{217}a_1c_2tanh(K)403a_1c_2tanh^2(K) + 755a_1c_2\right),\\ \varphi(x,t) &= -\left(\frac{9a_2\beta^2 - a_2\left(9\beta^2 + 28\sqrt[4]{2}\sqrt{f}\sqrt{\eta}\sqrt{\cos(t\omega)}\right)}{672\sqrt{2}a_1a_2c_2\eta}\right)\\ &\quad \left(4\sqrt{217}a_1c_2tanh(K) + a_1c_2\big(31tanch^2(K) + 21\big)\right), \end{aligned}$$

$$K = \frac{1}{6}\sqrt{\frac{31}{7}}\sqrt{\frac{a_1^2c_2^2}{a_2^2}}\Big(\frac{\sqrt{7}x\sqrt{a_2^2\left(9\beta^2\sqrt{f}\sqrt{\eta}\sqrt{\cos(t\omega)}+14\sqrt[4]{2}f\eta\cos(t\omega)\right)}}{6\,2^{3/8}a_1\beta c_2\sqrt{\kappa_1}\lambda}$$
$$+H(t)\Big),\ H(t)=\int_0^t \mu(s)\,ds;\mu(t)=\frac{\sqrt{9a_2^2\beta^2+64a_1^2c_2^2\kappa_1\lambda^2h(t)^2}-3a_2\beta}{8a_1c_2}, \tag{17}$$

where $h(t)$ is given in Eq. (16). It is worth mentioning the model equation in (8), in present section, exact solutions hold when $\kappa_2=\kappa_1$. In the next sections, we assume that $\kappa_2\neq\kappa_1$, so, only approximate solutions are derived.

3.2 Rational (approximate) solution

3.2.1 When $k=2$

The rational solution of Eq. (12) is expressed by,

$$r(z,t)=\frac{a_1\phi(z,t)+a_0}{s_1\phi(z,t)+s_0},\ \theta(z,t)=\frac{b_1\phi(z,t)+b_0}{s_1\phi(z,t)+s_0}, \tag{18}$$

together with auxiliary equations in Eq. (14). From (14), (18) into Eq. (12), and when a part of the coefficients of $\phi(z,\,t)^j,\ j=0,$ 1, 2, ...etc equal to zero leads to,

$$\begin{aligned}
\mu'(t)&=\frac{1}{c_0s_0(b_1s_0-b_0s_1)}\big(a_0b_0\eta s_0+2b_0c_0^2s_1^2\big(\kappa_2\lambda^2h(t)^2-\mu(t)^2\big)+fs_0^3\cos(t\omega)+b_1c_0s_0^2\big(c_1\kappa_2\lambda^2h(t)^2-\mu(t)(\beta+c_1\mu(t))\big)\\
&\quad+c_0s_0s_1\big(-\kappa_2\lambda^2(2b_1c_0+b_0c_1)h(t)^2+\mu(t)(b_0(\beta+c_1\mu(t))+2b_1c_0\mu(t))\big)\big),\\
b_1&=\frac{2a_0b_0s_1-a_1b_0s_0}{a_0s_0},\ h(t)=\frac{\sqrt{a_0s_1-a_1s_0}\sqrt{c_1s_1-2c_2s_0}\mu(t)}{\sqrt{\kappa_2\lambda^2(a_0s_1-a_1s_0)(c_1s_1-2c_2s_0)}},\\
c_0&=\frac{c_1s_0}{2s_1},\ c_1=\frac{c_2ms_0}{s_1},\quad a_0=\frac{n(a_1s_0)}{s_1},\ m=\frac{2n^2}{2n-1}.
\end{aligned} \tag{19}$$

The equation for $\mu'(t)$solves to,

$$\mu(t)=-\frac{2a_1\eta n^2}{\beta c_2ms_0-\beta c_2mns_0}+Ae^{-\beta t}+\frac{2fns_1(\beta\cos(t\omega)+\omega\sin(t\omega))}{b_0c_2m(n-1)\left(\beta^2+\omega^2\right)}. \tag{20}$$

Maximum error evaluation

It is worthy to mention that the non-zero coefficients or RTs are the errors. For an adequate choice of the parameters in the RSs as in what follows,

$$\begin{aligned}
n=1.1,s_1=0.5,b_0=0.3,s_0=0.5,\kappa_2=5,\kappa_1=5.001,\\
a_1=0.01,f=0.2,\eta=0.01,c_2=0.3,\beta=0.01,
\end{aligned} \tag{21}$$

the errors are given in Table 1.

In the Table 1, $\mu(t)$ is given in Eq. (20). The maximum error is shown in Fig. 2

The solutions of Eq. (12) are,

$$R(x,t)=\frac{P_1}{Q_1},\ P_1=a_1\Bigg(m-2n+\sqrt{(m-2)m}\tanh\Bigg(\frac{\sqrt{(m-2)m}(c_2s_0)}{2s_1}\frac{1}{\lambda\sqrt{a_1c_2\kappa_2(m-2)(n-1)}}$$
$$\Bigg(x\sqrt{a_1(n-1)}\sqrt{c_2(m-2)}\Bigg(-\frac{2a_1\eta n^2}{\beta c_2ms_0-\beta c_2mns_0}+Ae^{\beta(-t)}+\frac{2fns_1(\beta\cos(t\omega)+\omega\sin(t\omega))}{b_0c_2m(n-1)\left(\beta^2+\omega^2\right)}\Bigg)\Bigg)+H(t)\Bigg)\Bigg),$$

Table 1 The errors that result from inserting of Eq. (21) into the residue terms

$-1.5125000000000012\times10^{-6}-6\mu(t)+0.00183333\cos(t\omega)+0.00045121$
$1.5125000000005006\times10^{-10}\mu(t)^2-4.5375000000000036.\times10^{-6}\mu(t)+0.0055\cos(t\omega)+0.00143545$
$2.025\times10^{-10}\mu(t)^2-4.525000000000004\times10^{-6}\mu(t)+0.00548485\cos(t\omega)+0.00152098$
$1.5000000000000497\times10^{-10}\mu(t)^2-1.5000000000000013\times10^{-6}\mu(t)+0.00181818\cos(t\omega)+0.000536737$
$3.0028571665293494\times10^{-21}-0.000206612\cos(t\omega),\ 3.0028571665293494\times10^{-21}-0.000206612\cos(t\omega)$

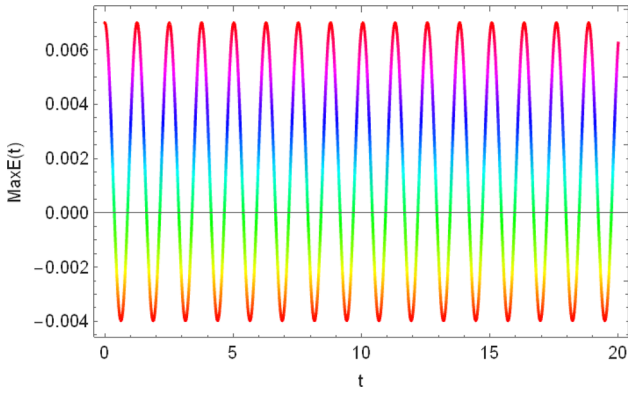

Fig. 2 By using Eq. (21). It shows that the maximum error is 6×10^{-3}

$$
\begin{aligned}
Q_1 &= s_1\Bigg[-2+m+\sqrt{(m-2)m}\tanh\Bigg(\frac{\sqrt{(m-2)m}(c_2 s_0)}{2s_1}\frac{1}{\lambda\sqrt{a_1 c_2 \kappa_2 (m-2)(n-1)}}\\
&\quad\left(x\sqrt{a_1(n-1)}\sqrt{c_2(m-2)}\left(-\frac{2a_1\eta n^2}{\beta c_2 m s_0-\beta c_2 m n s_0}+Ae^{\beta(-t)}+\frac{2fns_1(\beta\cos(t\omega)+\omega\sin(t\omega))}{b_0 c_2 m(n-1)\left(\beta^2+\omega^2\right)}\right)\right)+H(t)\Bigg)\Bigg],\\
(x,t) &= = \frac{P_2}{nQ_1},\ P_2 = b_0\Bigg[-2n+m(2n-1)+\sqrt{(m-2)m}(2n-1)\tanh\Bigg(\frac{\sqrt{(m-2)m}(c_2 s_0)}{2s_1}\frac{x\sqrt{a_1(n-1)}\sqrt{c_2(m-2)}}{\lambda\sqrt{a_1 c_2\kappa_2(m-2)(n-1)}}\\
&\quad\left(-\frac{2a_1\eta n^2}{\beta c_2 m s_0-\beta c_2 m n s_0}+Ae^{\beta(-t)}+\frac{2fns_1(\beta\cos(t\omega)+\omega\sin(t\omega))}{b_0 c_2 m(n-1)\left(\beta^2+\omega^2\right)}\right)+H(t)\Bigg)\Bigg],\\
H(t) &= -\frac{2a_1\eta n^2 t}{\beta c_2 m s_0-\beta c_2 m n s_0}+\frac{A-Ae^{\beta(-t)}}{\beta}+\frac{2fns_1(\beta\sin(t\omega)+\omega(-\cos(t\omega))+\omega)}{b_0 c_2 m(n-1)\omega\left(\beta^2+\omega^2\right)}.
\end{aligned}
\tag{22}
$$

The results in Eq. (22) are displayed 3D for $R(x,t)$ and $\varphi(x,t)$ in Fig. 3a (i)–(vi) and b(i)–(iv).

The 3D plot are represented for R, by varying the parameters η, β, κ_1 and f.

Figure 3a(iv), when compared Figs. (ii)–(vi) with Fig. 3a(i), we find that R varies significantly for increasing η, β, and f But there is no significant change for greater value of κ_1. Also, when comparing Fig. (iii) and (iv), we find that deformation in the DNA diameter when $\beta > 0.05$. On the other side, when comparing Fig. (v) and (vi), deformation occurs when $f > 0.25$.

The angle deviation $\varphi(x,t)$ is displayed in Fig. 3b(i)–(vi)

The 3D plot are represented for φ, by varying the parameters η, β, κ_1 and f.

Figure 3b(i)–(iv), when comparing. (ii)–(iv), we find that no significant change occurs in φ. when varying the parameters η,f and β.

3.2.2 When $k = 1$

Consider Eq. (13) and the auxiliary equations,

$$
\phi_z(z,t) = \lambda(c_1\phi(z,t)+c_0),\quad \phi_t(z,t) = \mu(t)(c_1\phi(z,t)+c_0). \tag{23}
$$

From Eq. (18) and (23) into Eq. (12) gives rise to,

$$
\begin{aligned}
\mu'(t) &= \frac{\kappa_2\lambda^2(c_1 s_0-2c_0 s_1)\,h(t)^2-s_0\mu(t)(\beta+c_1\mu(t))+2c_0 s_1\mu(t)^2}{s_0},\\
A''(t) &= \frac{a_0\eta\,A(t)^2}{s_0}+\frac{\frac{f s_0\cos(t\omega)}{\sigma}-2b_1 c_0\mu(t)\,A'(t)}{b_0}+A'(t)\left(\frac{2c_0 s_1\mu(t)}{s_0}-\beta\right),\\
A'(t) &= -\frac{1}{2a_0\beta s_0^2}\left(-\eta s_0 A(t)^2\left(2a_0^2-b_0^2\sigma^2\right)-\frac{2a_0 f s_0^3\cos(t\omega)}{b_0\sigma}+2c_0(a_1 s_0-a_0 s_1)A(t)\left((\kappa_1-\kappa_2)\lambda^2(c_1 s_0-2c_0 s_1)h(t)^2+\beta s_0\mu(t)\right)\right),\\
b_1 &= \frac{a_1 b_0}{a_0},\ h(t) = \frac{\sqrt{\beta}\sqrt{s_0}\sqrt{\mu(t)}}{\sqrt{(\kappa_1-\kappa_2)\left(-\lambda^2\right)(c_1 s_0-2c_0 s_1)}},\ a_0 = -\frac{b_0\sigma}{\sqrt{2}},\\
c_1 &= \frac{c_0 m s_1}{s_0},\quad a_1 = \frac{n(b_0\sigma s_1)}{s_0}.
\end{aligned}
\tag{24}
$$

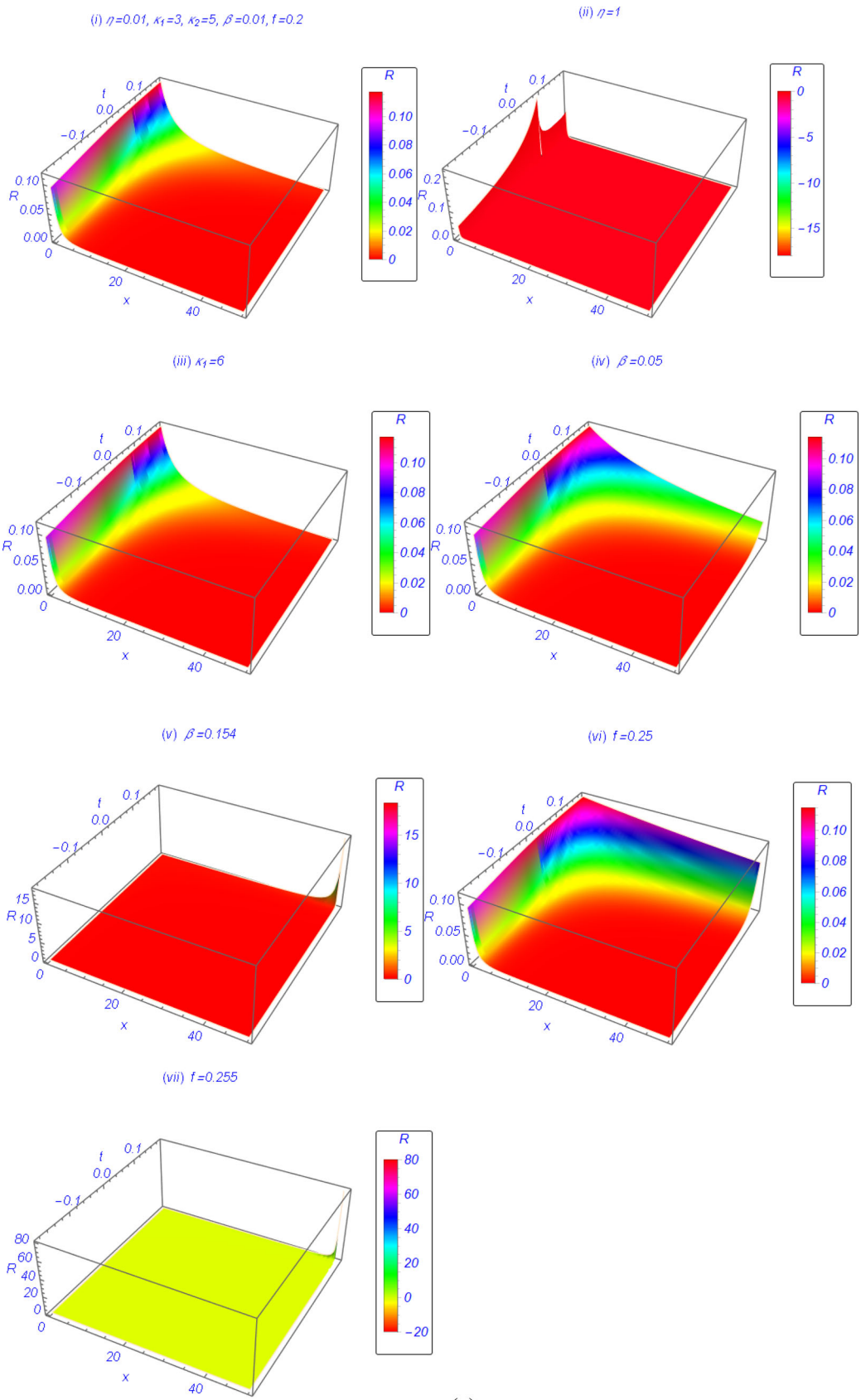

(a)

Fig. 3 **a** (i)–(iv) are displayed when $n = 1.1$, $s_1 = 0.5$, $b_0 = 0.3$, $s_0 = 0.5$, $\kappa_2 = 5$, $\kappa_1 = 5.001$, $a_1 = 0.01$, $f = 0.2$, $\eta = 0.01$, $c_2 = 0.3$, $\beta = 0.01$. **b** (i)–(iv). The caption as in Fig. 3a(i)–(vi) is used

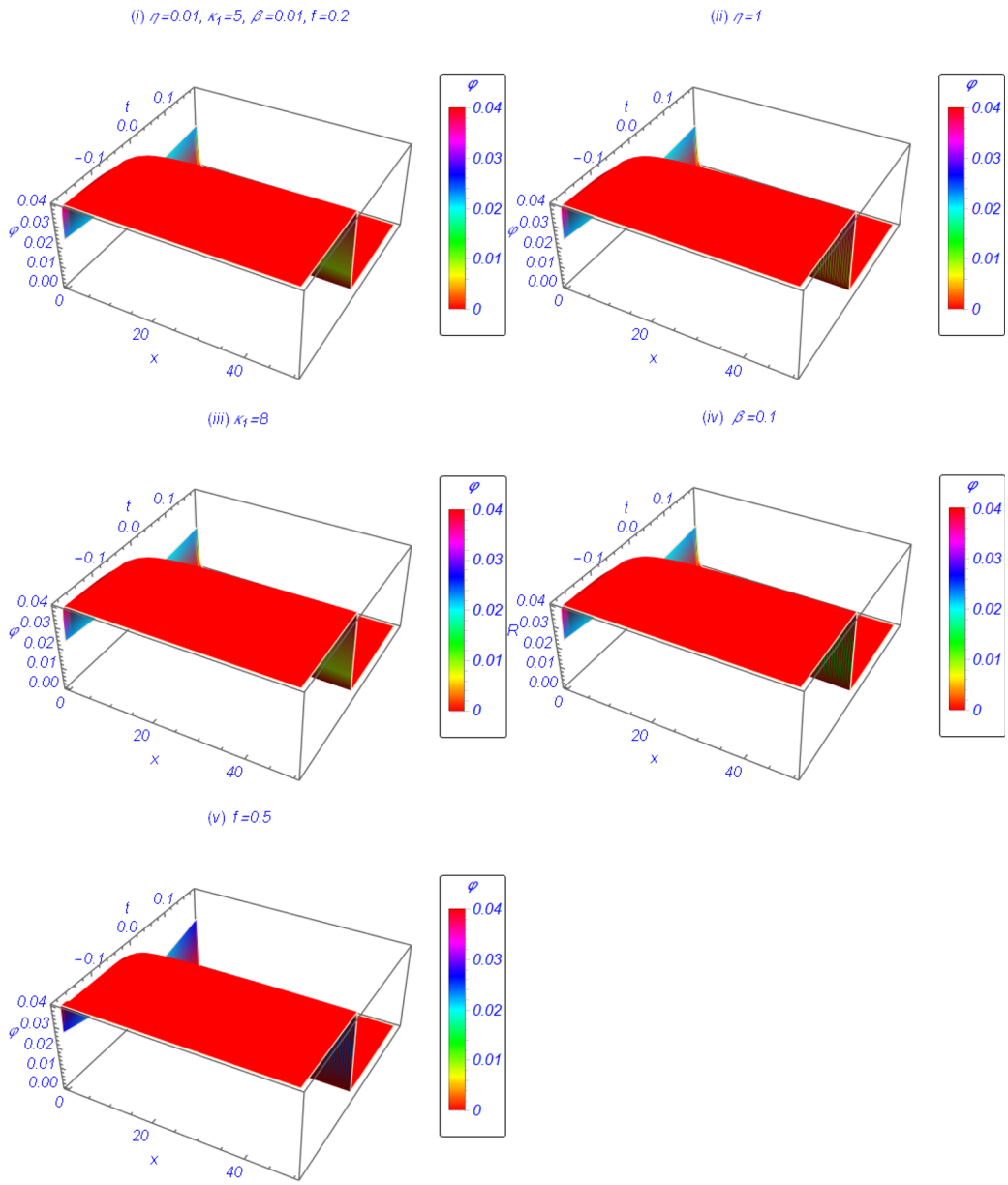

(b)

Fig. 3 continued

The compatibility equation, $(A'(t))'$-$A''(t) = 0$ leads to,

$$A(t) = \frac{\left(\sqrt[4]{2}\sqrt{s_0}\right)\sqrt{f\left(2\sqrt{2}a_1c_0s_0\mu(t)\cos(t\omega) + b_0\sigma\left(2c_0s_1\mu(t)\cos(t\omega) + s_0\omega\sin(t\omega)\right)\right)}}{b_0^{3/2}\sqrt{\beta}\sqrt{\eta}\sigma^{3/2}}. \tag{25}$$

The first equation in Eq. (24) integrates to,

$$\mu(t) = -\frac{\beta\kappa_1 s_0 e^{\beta\kappa_1 s_0\left(A-\frac{t}{(\kappa_1-\kappa_2)s_0}\right)}}{c_0\kappa_1(m-2)s_1 e^{\beta\kappa_1 s_0\left(A-\frac{t}{(\kappa_1-\kappa_2)s_0}\right)} + c_0\kappa_2(2-m)s_1 - 1}. \tag{26}$$

Maximum error evaluation

It is worth mentioning that the non-zero coefficients or RTs are the errors. For an adequate choice of the parameters in the rational solution as in what follows,

$$n = -0.7, \beta = 1.2, c_0 = 0.05, b_0 = 1.1, m = 2.1, s_1 = 0.5, \sigma = 3,$$

Table 2 The errors when inserting Eq. (27) into the residue terms

$0.0006\omega\sin(t\omega)+2.5707106781189444\times10^{-6}\mu(t)\cos(t\omega)$
$-1.7591518356795715\times10^{-6}-6\mu(t)(1.\mu(t)+1584.)\sqrt{0.0000707107\mu(t)\cos(t\omega)+1.2\omega\sin(t\omega)}$
$0.000499646\omega\sin(t\omega)-1.539257856219625\times10^{-6}\mu(t)^2\sqrt{0.0000707107\mu(t)\cos(t\omega)+1.2\omega\sin(t\omega)}$
$+\mu(t)\left(-0.00243818\sqrt{0.0000707107\mu(t)\cos(t\omega)+1.2\omega\sin(t\omega)}-9.316095268233119\times10^{-6}\cos(t\omega)\right)$
$0.000104019\omega\sin(t\omega)-4.3280102989382175\times10^{-6}\mu(t)\cos(t\omega)$
$-2.500000000000368\times10^{-8}\mu(t)\cos(t\omega)-0.000424264\omega\sin(t\omega)-1.7927669529665738\times10^{-6}\cos(t\omega)$
$(1.\mu(t)+283.984)+1.2439081921457883\times10^{-6}\mu(t)(1.\mu(t)+1008.)$
$\sqrt{0.0000707107\mu(t)\cos(t\omega)+1.2\omega\sin(t\omega)}$

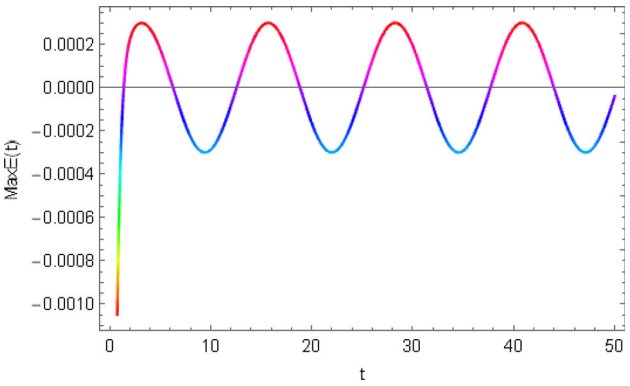

Fig. 4 By using Eq. (27, it shows that the absolute maximum error is 1×10^{-3}

$$s_0=1.2,\kappa_2=0.7,\kappa_1=1.1,f=0.5,\eta=0.3,\omega=0.5,A=1.2, \tag{27}$$

the errors (RTs) are given in Table 2.

In the Table 2, $\mu(t)$ is given in Eq. (26). The maximum error is shown in Fig. 4

The solution of Eq. (12) are,

$$\begin{aligned}
R(x,t)&=-\frac{1}{2^{3/4}Q}\left[\sqrt{b_0}\sqrt{\sigma}(-2nAms_1e^{(\frac{c_0ms_1}{s_0}(\frac{\sqrt{\beta}\sqrt{s_0}x\sqrt{\mu(t)}}{\sqrt{c_0(\kappa_1-\kappa_2)\lambda^2(-(m-2))s_1}}+H(t)))}+\sqrt{2}ms_0+2n)\sqrt{\frac{f\left(2c_0\left(\sqrt{2}n+1\right)s_1\mu(t)\cos(t\omega)+s_0\omega\sin(t\omega)\right)}{\beta b_0\sigma}}\right],\\
\varphi(x,t)&=\frac{1}{Q}\left[\sqrt[4]{2}\sqrt{b_0}\sqrt{\sigma}\left(ms_0-\sqrt{2}n\left(Ams_1e^{(\frac{c_0ms_1}{s_0}(\frac{\sqrt{\beta}\sqrt{s_0}x\sqrt{\mu(t)}}{\sqrt{c_0(\kappa_1-\kappa_2)\lambda^2(-(m-2))s_1}}+H(t)))}-1\right)\right)\sqrt{\frac{f\left(2c_0\left(\sqrt{2}n+1\right)s_1\mu(t)\cos(t\omega)+s_0\omega\sin(t\omega)\right)}{\beta b_0\sigma}}\right],\\
Q&=\sqrt{\eta}\sqrt{s_0}\left(Ams_1e^{(\frac{c_0ms_1}{s_0}(\frac{\sqrt{\beta}\sqrt{s_0}x\sqrt{\mu(t)}}{\sqrt{c_0(\kappa_1-\kappa_2)\lambda^2(-(m-2))s_1}}+H(t)))}+ms_0-1\right).
\end{aligned} \tag{28}$$

The results in Eq. (28) are displayed in Fig. 5(i)–(iii)

The 3D plot, contour plot and for different values of t. Fig 5(iii), shows Cavity soliton. Figure 5a(iii) shows

4 General case

Here, φ is taken free. So, the transformation $\varphi=\arctan\left(\frac{1}{2}(v-\frac{1}{v})\right)$ is introduced into Eq. (8) (or into Eq. (9)) and we have,

$$\begin{aligned}
&\left(v(x,t)^2+1\right)(R_{tt}(x,t)-\kappa_1R_{xx}(x,t))+2\eta v(x,t)-\eta\left(v(x,t)^2+1\right)=0,\\
&\left(v(x,t)^2+1\right)v_{tt}(x,t)-\frac{1}{2}\eta\,R(x,t)\left(v(x,t)^2-1\right)^3+2v(x,t)\left(\beta\left(v(x,t)^2+1\right)v_t(x,t)\right.\\
&\left.+\kappa_2\left(2v(x,t)v_x(x,t)^2-\left(v(x,t)^2+1\right)v_{xx}(x,t)\right)-2v(x,t)v_t(x,t)^2\right)\\
&-f\cos(t\omega)v(x,t)\left(v(x,t)^2+1\right)^2=0.
\end{aligned} \tag{29}$$

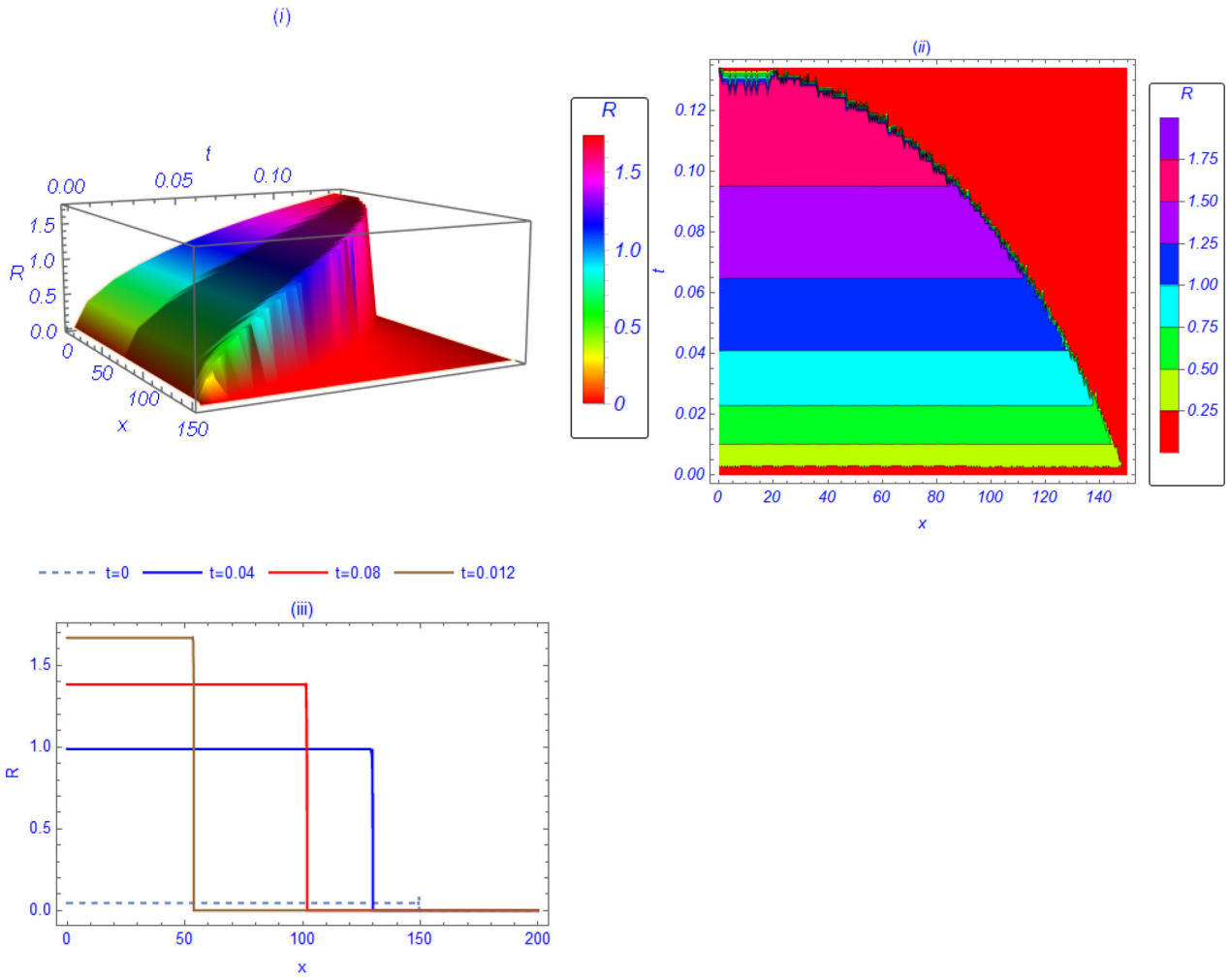

(a)

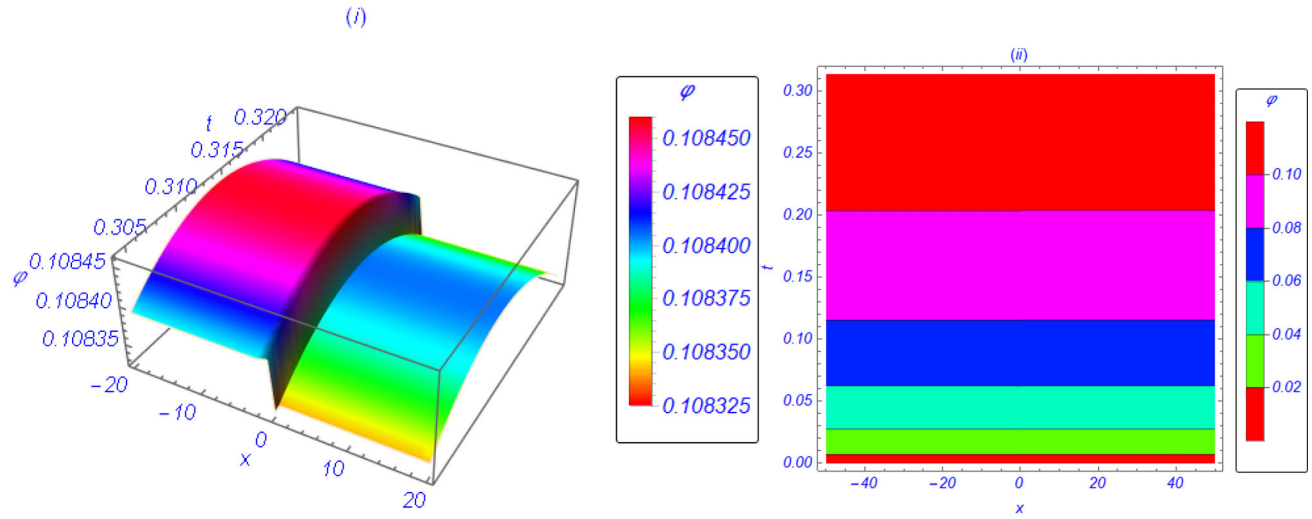

(b)

Fig. 5 **a**(i)–(iii) are displayed by using Eq. (27) ($n = -0.7$, $\beta = 1.2$, $c_0 = 0.05$, $b_0 = 1.1$, $m = 2.1$, $s_1 = 0.5$, $\sigma = 3$, $s_0 = 1.2$, $\kappa_2 = 0.7$, $\kappa_1 = 1.1$, $f = 0.5$, $\eta = 0.3$, $\omega = 0.5$, $A = 1.2$. **b** (i), (ii) show 3D and contour plot of φ at the same caption of 5a(i)–(iii)

Table 3 The errors from plugging Eq. (34) in the residue terms

$0.168\mu(t)^2 + 0.00519885\cos(t\omega) - 0.0000372998$
$0.1323\mu(t)^2 - 0.00686375\cos(t\omega) - 0.0000408462$
$-0.304555\mu(t)^2 + 0.00567713\cos(t\omega) + 0.0000304702$
$-0.240138\mu(t)^2 + 0.00247206\cos(t\omega) + 0.0000180777$
$0.0114629\mu(t)^2 + 0.000941555\cos(t\omega) + 1.0335937499999998 \times 10^{-7}$

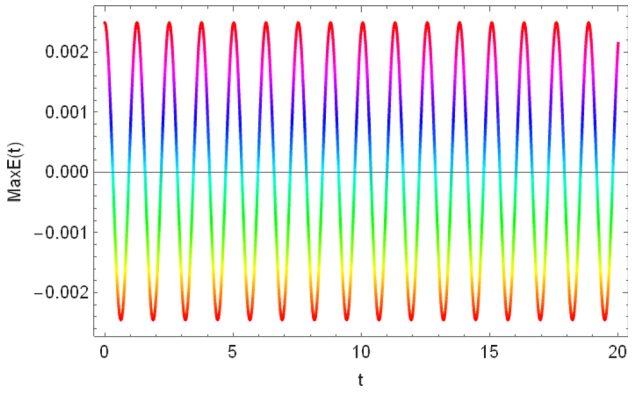

Fig. 6 Is displayed by using Eq. (34). The absolute maximum error is 2×10^{-3}

In Eq. (29), the transformations $R(x,\,t) = r(z,\,t),\;\; v(x,\,t) = V(z,\,t),\;\; z = h(t)x$, and $t = t$, are introduced. Thus Eq. (29) becomes,

$$\begin{aligned}
&\big(V(z,t)^2+1\big)\big(r_{tt}(z,t)-\kappa_1 h(t)^2 r_{zz}(z,t)\big)+2\eta V(z,t)-\eta\big(V(z,t)^2+1\big)=0,\\
&\big(V(z,t)^2+1\big)V_{tt}(z,t)-\frac{1}{2}\eta r(z,t)\big(V(z,t)^2-1\big)^3+2V(z,t)\big(\beta\big(V(z,t)^2+1\big)V_t(z,t)\\
&+\kappa_2 h(t)^2\big(2V(z,t)V_z(z,t)^2-\big(V(z,t)^2+1\big)V_{zz}(z,t)\big)-2V(z,t)V_t(z,t)^2\big)\\
&-f\cos(t\omega)V(z,t)\big(V(z,t)^2+1\big)^2=0.
\end{aligned} \tag{30}$$

4.1 Solutions of Eq. (29)

Here, the polynomial solutions take the form,

$$\begin{aligned}
&r(z,t)=a_2\phi(z,t)^2+a_1\phi(z,t)+a_0,\;\; V(z,t)=b_2\phi(z,t)^2+b_1\phi(z,t)+b_0,\\
&b_0=\frac{a_0 b_2}{a_2},\;\; b_1=\frac{a_1 b_2}{a_2},
\end{aligned} \tag{31}$$

together with the auxiliary Eq. (14), and we have,

$$\begin{aligned}
&a_0=-\frac{a_1^2}{3a_2},\;\; h(t)=\frac{\sqrt{-6a_2^3\big(b_2 f\cos(t\omega)+4c_2^2\mu(t)^2\big)-7a_1^4b_2^2\eta+9a_2^4\eta}}{2\sqrt{13}a_1\sqrt{a_2}c_1c_2\sqrt{\kappa_2}\lambda},\\
&b_2=\frac{3a_2^2}{\sqrt{7}a_1^2},\;\; c_0=\frac{-12a_1^3c_1c_2-13a_2a_1^2c_1^2}{6a_2^3},\;\; a_2=a_1c_1m,\;\; c_2=-\frac{13}{12}c_1^2m,\\
&\mu'(t)=\frac{18\sqrt{7}a_2a_1c_2f\cos(t\omega)-18\sqrt{7}a_2^2c_1f\cos(t\omega)-7a_1^2c_2(33a_1\eta+8\beta c_2\mu(t))}{56a_1^2c_2^2}.
\end{aligned} \tag{32}$$

The last equation in Eq. (32) integrates to,

$$\mu(t)=\frac{9009a_1\eta}{2366\beta c_1^2m}+\frac{2\Big(1183Ac_1e^{-\beta t}-\frac{675\sqrt{7}f(\beta\cos(t\omega)+\omega\sin(t\omega))}{\beta^2+\omega^2}\Big)}{2366c_1}. \tag{33}$$

The errors (RTs), by taking,

$$\eta=0.005, a_1=0.002, m=-0.5, c_1=0.7, \kappa_2=1.5, \kappa_1=1.4, \beta=0.3, f=0.02, A=0.001, \tag{34}$$

are given in Table 3,

Where $\mu(t)$is given in Eq. (33).The maximum error is shown in Fig. 6

Finally, the solutions of Eq. (29) are,

$$
\begin{aligned}
R(x,t) &= \frac{1}{507c_1^2 m}\left(a_1 450\tanh\left[\frac{1}{61516c_1^2\sqrt{\kappa_2}\lambda(a_1c_1m)^{3/2}}\left(c_1\left(-1092\sqrt{78}x\sqrt{K}+30758c_1^2\sqrt{\kappa_2}\lambda H(t)(a_1c_1m)^{3/2}\right)\right)\right]\right.\\
&\left.+c_1\left(173+108\tanh\left[\frac{1}{61516c_1^2\sqrt{\kappa_2}\lambda(a_1c_1m)^{3/2}}\left(c_1\left(-1092\sqrt{78}x\sqrt{K}+30758c_1^2\sqrt{\kappa_2}\lambda H(t)(a_1c_1m)^{3/2}\right)\right)\right]\right)^2\right),\\
v(x,t) &= \frac{1}{169\sqrt{7}c_1}\left(450c_1\tanh\left[\frac{c_1}{61516c_1^2\sqrt{\kappa_2}\lambda(a_1c_1m)^{3/2}}\left(-1092\sqrt{78}x\sqrt{K}+30758c_1^2\sqrt{\kappa_2}\lambda H(t)(a_1c_1m)^{3/2}\right)\right]\right.\\
&\left.+c_1\left(173+108\tanh\left[\frac{1}{61516c_1^2\sqrt{\kappa_2}\lambda(a_1c_1m)^{3/2}}\left(c_1\left(-1092\sqrt{78}x\sqrt{K}+30758c_1^2\sqrt{\kappa_2}\lambda H(t)(a_1c_1m)^{3/2}\right)\right)\right]^2\right)\right)\right),\\
K &= -m^3a_1^3c_1^3\left[\frac{3c_1^2fm^2\cos(t\omega)}{\sqrt{7}}+\frac{1}{1192464\beta^2\left(\beta^2+\omega^2\right)^2}\left(e^{-2\beta t}\left(9009a_1\eta\left(\beta^2+\omega^2\right)e^{\beta t}\right.\right.\right.\\
&\left.\left.\left.+2m\beta c_1(-675\sqrt{7}fe^{\beta t}(\beta\cos(t\omega)+\omega\sin(t\omega))\ 1183Ac_1\left(\beta^2+\omega^2\right))\right)^2\right],\\
\varphi(x,t) &= \tan^{-1}\left(\frac{1}{2}\left(v(x,t)-\frac{1}{v(x,t)}\right)\right),\\
H(t) &= \frac{99a_1\eta t}{26\beta c_1^2 m}+\frac{A-Ae^{-\beta t}}{\beta}-\frac{675f(\beta\sin(t\omega)+\omega(-\cos(t\omega))+\omega)}{169\sqrt{7}c_1\omega\left(\beta^2+\omega^2\right)}.
\end{aligned}
\tag{35}
$$

The results in Eq. (35) are displayed in Fig. 7

5 Velocity and heating of DNA

Genome size refers to the amount of DNA contained in a haploid genome expressed either in terms of the number of base pairs, kilo-bases ($1kb = 1000bp$), or as the mass of DNA in picograms ($1\,pg = 10^{-12}g$). Genome, for a human contains about 3 billion bases (3×10^9) and about 20,000 genes on 23 pairs of chromosomes. Each base pair measures approximately $340pm$, which means 340 picometers. A picometer is equal to 1×10^{-12} meters. The velocity is defined by,

$$
v(t) = \frac{Nl_0\int_R \mid R(\bar{x},t)_t \mid \mathrm{d}\bar{x}}{\int_R \mid R(\bar{x},t)_{\bar{x}} \mid \mathrm{d}\bar{x}}, \quad \bar{x} = \frac{x}{Nl_0},
\tag{36}
$$

where, $N = 3 \times 10^9$and $l_0 = 3.4 \times 10^{-10}$ m. By considering the results in Eq. (17), the velocity is displayed In Fig. 8

The temperature of DNA due to the presence of microwave (MW) is estimated. MW is an electromagnetic wave with a relatively long wavelength and low frequency. To this issue, the Boltzmann equation is used,

$$
K_{\mathrm{B}}\mathrm{T}=\frac{m_0Nl_0^2}{2} < v^2 >,
\tag{37}
$$

where, $m_0 = 10^{-12}g = 10^{-15}$Kg, T is the temperature, and K_{B} is the Boltzmann constant ($K_{\mathrm{B}} = 1.38 \times 10^{-23}$ Kgm^2 K^{-1} s^{-2}), and,

$$
< v^2 >= \frac{\int_{R^+}\int_{\mathbb{R}}(\mid R(\bar{x},t)_t \mid)^2\mathrm{d}\bar{x}\mathrm{d}t}{\int_{R^+}\int_{\mathbb{R}}(\mid R(\bar{x},t)_{\bar{x}} \mid)^2\mathrm{d}\bar{x}\mathrm{d}t}, \ \bar{x} = \frac{x}{Nl_0}.
\tag{38}
$$

From Eq. (38) the temperature is $T = 82.8$ K.

6 Stability of the initial value problem

Here, a study of the stability of the DNA dynamics in the presence of microwave is carried. This study can help to depict if the DNA molecules can be damaged or not, which depends on stability (or instability of the motion of DNA molecules. It is known scientifically that, the energy of microwaves is not sufficient to break a chemical bond in DNA, but genotoxic effects may occur by indirect mechanisms via generation of oxygen free radicals or a disturbance in DNA-repair processes.

Here, the stability of initial value problem is considered. To this issue, assume that

$\frac{\partial^2 R(x,t)}{\partial t^2} \mid_{t=0} = 0$, $\frac{\partial^2 \varphi(x,t)}{\partial t^2} \mid_{t=0} = 0$, $\frac{\partial \varphi(x,t)}{\partial t} \mid_{t=0} = 0$, $R(x,\,0) = R_0(x)$,

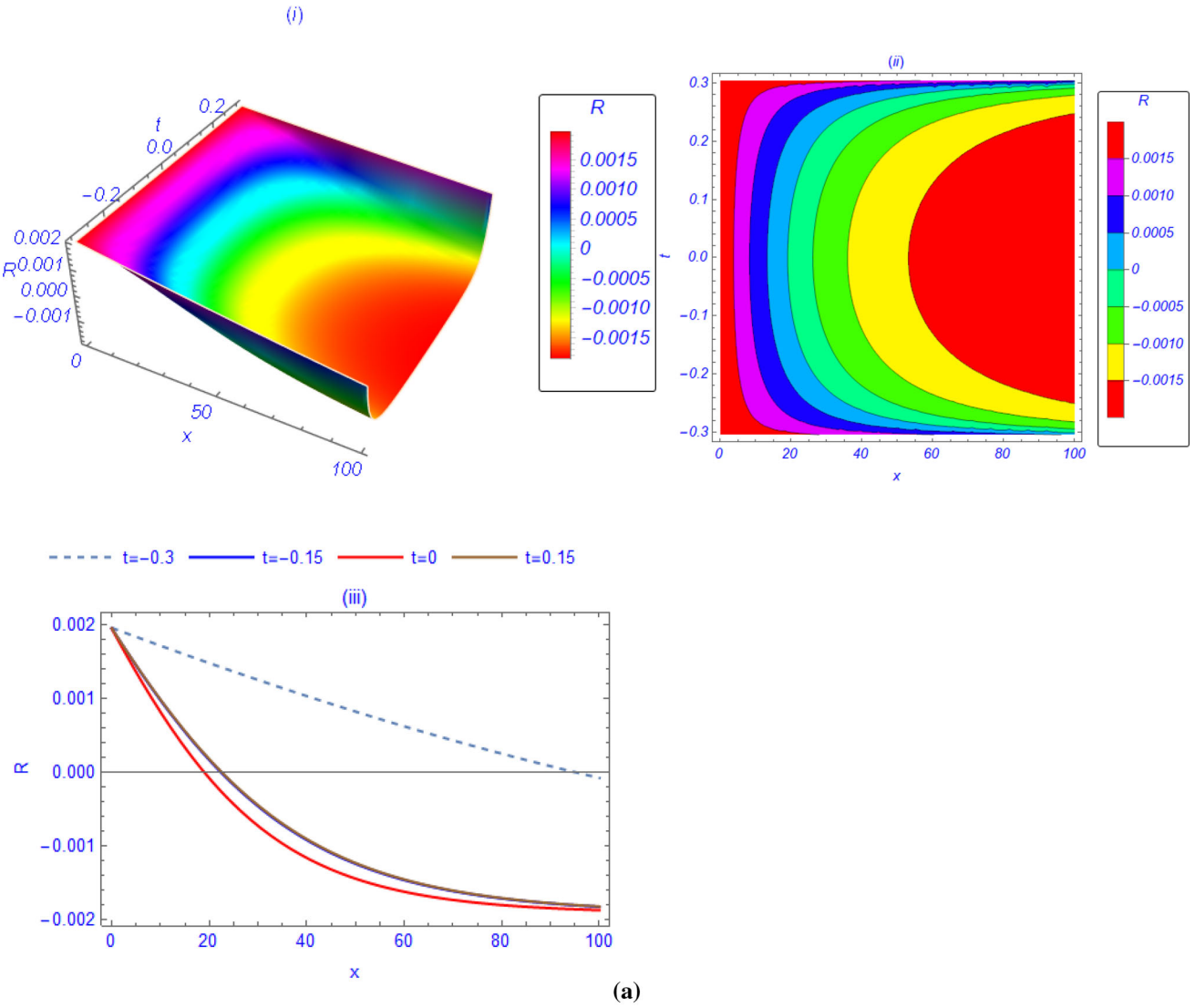

(a)

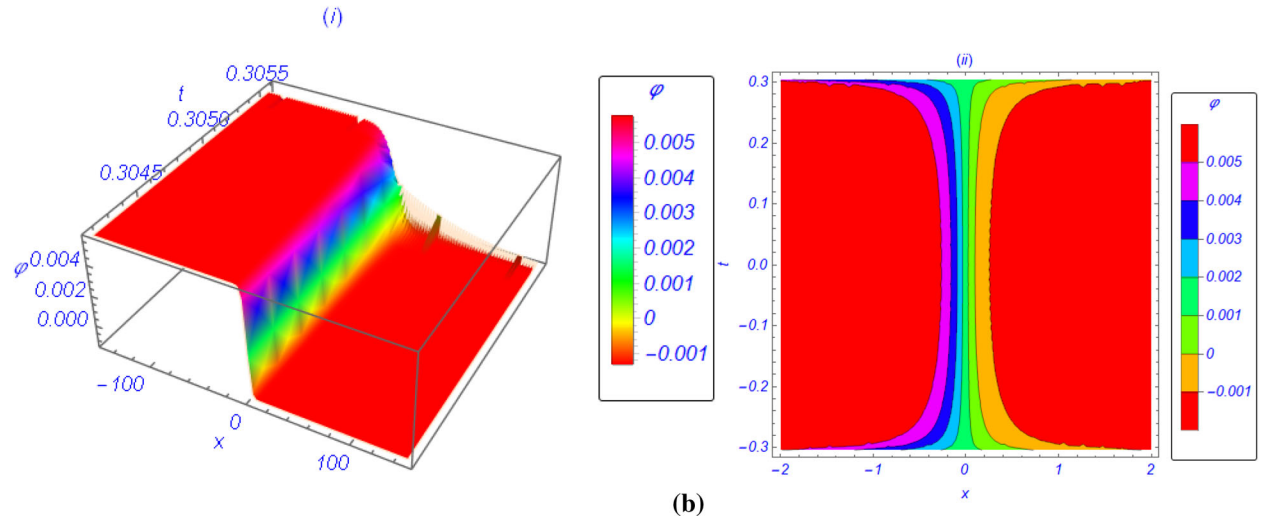

(b)

Fig. 7 **a**(i)–(iii) are displayed when $\eta = 0.005$, $a_1 = 0.002$, $m = -0.5$, c_1:==0.7, , $\kappa_2 = 1.5$, $\kappa_1 = 1.4$, $\beta = 0.3$, $f = 0.02$, $A = 0.001$. **b** (i), (ii) show 3D and contour plot of φ at the same caption of 7a(i)–(iii)

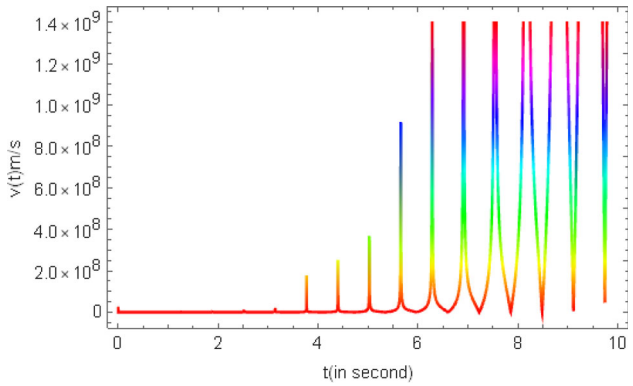

Fig. 8 The velocity is displayed against t for the parameters in Eq. (34)

and $\varphi(x,\,0) = \varphi_0(x)$. So, in this case Eq. (8) reduces to,

$$\begin{aligned} -\kappa_1 \frac{\partial^2 R_0(x)}{\partial x^2} - \eta\,(1 - \cos(\varphi_0(x))) = 0, \\ -\kappa_2 \frac{\partial^2 \varphi_0(x)}{\partial x^2} - f - \eta R_0(x)\sin(\varphi_0(x)) = 0. \end{aligned} \tag{39}$$

Eq. (39) describes the solutions of the initial values. For simplicity, in Eq. (39), we take $\sin(\varphi_0(x)) \simeq \varphi_0(x)$ and $\cos(\varphi_0(x)) \simeq 1 - \frac{\varphi_0(x)^2}{2}$, so, Eq. (39) becomes,

$$-\kappa_1 \frac{\partial^2 R_0(x)}{\partial x\,\partial x} - \frac{1}{2}\eta\varphi_0(x)^2 = 0, \quad -\kappa_2 \frac{\partial^2 \varphi_0(x)}{\partial x\,\partial x} - f - \eta R_0(x)\varphi_0(x) = 0. \tag{40}$$

Eq. (40) are solved by the same method in the above and we get the exact solutions,

$$\begin{aligned} R_0(x) &= \frac{\sqrt{\frac{2f}{\sqrt{3}} + f}\,\sqrt[4]{\kappa_2}}{2^{3/4}\sqrt{\eta}\,\sqrt[4]{\kappa_1}}\left(-3\tanh^2\left(\frac{\sqrt[4]{\frac{2f}{\sqrt{3}} + f}\,\sqrt[4]{\eta}x}{2^{7/8}\sqrt[8]{\kappa_1}\kappa_2^{3/8}}\right) - \sqrt{3} + 4\right), \\ \varphi_0(x) &= \frac{\sqrt{\frac{2f}{\sqrt{3}} + f}\,\sqrt[4]{\kappa_1}}{\sqrt[4]{2}\sqrt{\eta}\,\sqrt[4]{\kappa_2}}\left(3\tanh^2\left(\frac{\sqrt[4]{\frac{2f}{\sqrt{3}} + f}\,\sqrt[4]{\eta}x}{2^{7/8}\sqrt[8]{\kappa_1}\kappa_2^{3/8}}\right) - \sqrt{3}\right). \end{aligned} \tag{41}$$

Now, we use the perturbation expansion,

$$R(x,t) = R_0(x) + \epsilon_1 u(x,t), \quad \varphi(x,t) = \varphi_0(x) + \epsilon_2 v(x,t), \tag{42}$$

into Eq. (8) we get the equation,

$$\begin{gathered} M\begin{pmatrix}\epsilon_1\\ \epsilon_2\end{pmatrix},\ M = \begin{pmatrix}a_{11} & a_{12}\\ a_{21} & a_{22}\end{pmatrix}, \\ a_{11} = u_{tt}(x,t) - \kappa_1 u_{xx}(x,t),\ a_{12} = -\eta\varphi_0(x)u(x,t),\ a_{21} = -\eta\varphi_0(x)v(x,t), \\ a_{22} = -\eta R_0(x)v(x,t) + \beta v_t(x,t) - \kappa_2 v_{xx}(x,t) + v_{tt}(x,t) - f\cos(t\omega). \end{gathered} \tag{43}$$

Eq. (43) solves to $det(M) = 0$, which leads to,

$$\begin{gathered} -\eta^2\varphi_0(x)^2 u(x,t)v(x,t) - (u_{tt}(x,t) - \kappa_1 u_{xx}(x,t)) \\ \eta R_0(x)v(x,t) - \beta v_t(x,t) + \kappa_2 v_{xx}(x,t) - v_{tt}(x,t) + f\cos(t\omega) = 0. \end{gathered} \tag{44}$$

The Eq. (44) is solved when subjected to the boundary conditions (BCs) are, $|\,u(\pm\infty,\,t)\,| < K_1$ and $|\,v(\pm\infty,\,t)\,| < K_2$. It is worth mentioning that, the solutions in Eq. (41) verifies these conditions. To discuss the stability of the solution in Eq. (41), a solution of Eq. (44) has to be derived, which is not amenable. So, consider the following theorem.

Theorem 1 *The solutions of Eq. (39) that satisfy the aforementioned BCs are unstable.*

Proof. Assume the contraction, that is the solutions of Eq. (44) are stable. That is, they are periodic in time. Now take,

$$u_{tt}(x,\,t) - \kappa_1 u_{xx}(x,\,t) = mu(x,\,t),$$

which gives rise to,

$$u(x,t) = \cos(hx - ct),\ m = -c^2 + h^2\kappa_1, \tag{45}$$

Assume that $v(x,\,t) = V(x)\cos(t\omega)$*, it is found that Eq. (44) reduces to,*

$$\xi^2\left(d-\xi^2 r\right)+\left(1-\xi^2\right)\frac{\partial}{\partial\xi}\left(\left(1-\xi^2\right)\frac{\partial Q(\xi)}{\partial\xi}\right)=0,$$

$$r=-\frac{3\left(2\sqrt{3}+3\right)f\eta\sqrt{\kappa_1}}{\sqrt{2}\sqrt{\kappa_2}},d=-\frac{3c^2\sqrt{\frac{2f}{\sqrt{3}}+f}\sqrt{\eta}\sqrt[4]{\kappa_2}}{2^{3/4}\sqrt[4]{\kappa_1}}+\frac{\left(2\sqrt{3}+3\right)\sqrt{6}f\eta\sqrt{\kappa_1}}{\sqrt{\kappa_2}}+\frac{3\sqrt{\frac{2f}{\sqrt{3}}+f}\sqrt{\eta}h^2\kappa_1^{3/4}\sqrt[4]{\kappa_2}}{2^{3/4}}. \tag{46}$$

The Eq. (46) solved to,

$$\begin{aligned}Q(\xi)=k+\frac{1}{24}\big(&4c\xi^2+4log(1-\xi)(-3d+3k+4r)+3(r-d)log^2(1-\xi)\\&4log(\xi+1)(4c-3(d+g))-6log(2)\,(c-d)log(\xi+1)-6log(2)\,(r-d)log(\xi-1)\\&+3(c-d)log^2(\xi+1)+6(c-d)Li_2\left(\frac{1-\xi}{2}\right)+6(c-d)Li_2\left(\frac{\xi+1}{2}\right)\big),\end{aligned} \tag{47}$$

where k and g are arbitrary parameters and Li_2*is the logarithmic integral of the second kind,* $Li_2(x)=\int_2^x\frac{dt}{lnt}$.

Indeed, the solution in Eq. (47) is unbounded, so, the BCs are not satisfied. This complete the proof □.

From Theorem 1, it is concluded that, in the dynamics of DNA molecules exposed to microwave, molecules, deformation can occur.

7 Conclusions

The extended unified method is used to find these solutions, and the errors in the approximate solutions are controlled by choosing suitable parameters in the residue terms. The results of this model are typically displayed graphically, which can provide a visual understanding of the dynamics at play.

One of the key findings of this model is that the DNA diameter varies significantly depending on the strength of the hydrogen bond, the decaying rate, and the microwave amplitude. It is also observed that deformation in the DNA occurs when the damping rate and the microwave amplitude exceed a critical value. The stability of the initial value problem is analyzed in this model, and it is found that the solution is unstable, which impacts DNA deformation. This instability could have significant implications for our understanding of DNA structure and function. For a more detailed understanding, you may want to look into resources that delve into the structural features of the DNA double helix and their effects on its elastic mechanical properties. There are also studies that discuss the mathematics of DNA structure, mechanics, and dynamics. These resources might provide more insights into the continuum model for the dynamics of torsional DNA molecules. The major conclusion from this model is the recommendation to avoid exposure to microwaves, especially when they are of high amplitudes. This is an important consideration for maintaining the integrity of DNA structures.

Author contributions Wrote the paper, conceptualization, and revision.

Funding Open access funding provided by The Science, Technology & Innovation Funding Authority (STDF) in cooperation with The Egyptian Knowledge Bank (EKB).

Data availability There is no data set used.

Declarations

Conflict of interest The author declares that there is no Conflict of interest.

Ethical approval The author declares that there is n animal studies in this work

Open Access This article is licensed under a Creative Commons Attribution 4.0 International License, which permits use, sharing, adaptation, distribution and reproduction in any medium or format, as long as you give appropriate credit to the original author(s) and the source, provide a link to the Creative Commons licence, and indicate if changes were made. The images or other third party material in this article are included in the article's Creative Commons licence, unless indicated otherwise in a credit line to the material. If material is not included in the article's Creative Commons licence and your intended use is not permitted by statutory regulation or exceeds the permitted use, you will need to obtain permission directly from the copyright holder. To view a copy of this licence, visit http://creativecommons.org/licenses/by/4.0/.

References

1. M. Bates, M. Burns, A. Meller, Biophys. J. **84**, 2366 (2003)

2. J.S. Hur, E.S.G. Shaqfeh, H.P. Babcock, S. Chu, Phys. Rev. E **66**, 011915 (2002)
3. C.G. Baumann, V.A. Bloomfield, S.B. Smith, C. Bustamante, M.D. Wang, S.M. Block, Biophys. J. **78**(4), 1965 (2000)
4. P.K. Wong, Y.-K. Lee, C.-M. Ho, J. Fluid Mech. **497**, 55 (2003)
5. X.-D. Yang, R.V.N. Melnik, Comput. Bio. Chem. **31**(2), 110 (2007)
6. B.S. Alexandrov, L.T.W.K.Ø. Rasmussen, A.R. Bishop, K.B. Blagoev, Phys. Rev. E **74**, 05090 (2026)
7. D. Hennig, J.F.R. Archilla, Phys. A: Statist. Mech. Appl. **331**(3–4), 579 (2004)
8. K. Ott, L. Martini, J. Lipfert, U. Gerland, Biophys. J . **118**, 1690 (2020)
9. S. Srivastava, Y. Singh, Eur. Lett. **85**(3), 8001 (2009)
10. D. Panja, G.T. Barkema, J.M.J. van Leeuwen, Phys. Rev. E **93**, 042501 (2016)
11. M. Zoli, Eur. Biophys. J. **51**, 431 (2022)
12. A. Borkar, I. Ghosh, D. Bhattacharyya, J. Biomol. Struct. Dyn. **27**(5), 695 (2012)
13. M. Saha, T.C. Kofané, Phys. Scr. **89**, 085003 (2014)
14. S. Ma, Z. Rong, C. Liu, X. Qin, X. Zhang, Q. Che, Cell Biol. **220**(2), e201911025 (2021)
15. S.E. Polo, S.P. Jackson, Genes Dev. **25**(5), 409 (2011)
16. J.M. Kim, Int. J. Mol. Sci. **23**(13), 6986 (2022)
17. S. Jaiswal, X. Han, H.P. Lu, Phys. Chem. B **126**(5), 997 (2022)
18. M.M. Heldring, L.S. Wijaya, M. Niemeijer, H. Yang, T. Lakhal, S.E. Le Dévédec, B. van de Water, J.B. Beltman, PLoS Comput. Biol. **18**(7), e1010264 (2022)
19. H.I. Abdel-Gawad, M. Tantawy, T.N. Nkomom, J.B. Okaly, Phys. Scr. **96**(12), 125246 (2021)
20. A.R. Seadawy, M. Bilal, M. Younis, S.T.R. Rizvi, S. Althobaiti, M.M. Makhlouf, Chaos, Solitons Fractals **144**, 110669 (2021)
21. W. Alka, A. Goyal, C.N. Kumar, Phys. Lett. A **375**(3), 480 (2011)
22. C.B. Tabi, A. Mohamadou, T.C. Kofané, Chin. Phys. Lett. **26**, 068703 (2009)
23. G. Gaeta, L. Venier, J. Nonlinear Math. Phys. **15**(2), 186 (2008)
24. E. Skoruppa, S.K. Nomidis, J.F. Marko, E. Carlon, Phys. Rev. Lett. **121**, 088101 (2018)
25. E.H.M. Zahran, A. Bekir, Mod. Phys. Lett. B **37**(13), 2350027 (2023)
26. H.I. Abdel-Gawad, M. Tantawy, Appl. Math. Inf. Sci. Lett. **6**(2), 85 (2018)
27. A. Svidlov, M. Drobotenko, A. Basov, E. Gerasimenko, V. Malyshko, A. Elkina, M. Baryshev, S. Dzhimak, Int. J. Mol. Sci. **22**(15), 7873 (2021)
28. A. Sulaiman, F.P. Zen, H. Alatas, T. Handoko, Phys. D: Nonlinear Phenom. **241**(19), 1640 (2012)
29. C.L. Gninzanlong, F.T. Ndjomatchoua, C. Tchawoua, Phys. Rev. E **99**, 052210 (2019)
30. V. Vasumathi, M. Daniel, Phys. Lett. A **373**, 76 (2008)
31. M. Daniel, V. Vasumathi, Phys. Lett. A **372**, 5144 (2008)
32. C.B. Tabi, A. Mohamadou, T.C. Kofan, Phys. Lett. A **373**, 2476 (2009)
33. F. Dominguez Adame, A. Sanchez, Y.S. Kivshar, Phys. Rev. E **52**, R2183 (1995)
34. A. Svidlov, M. Drobotenko et al., Int. J. Mol. Sci. **22**, 7873 (2021)
35. H.I. Abdel Gawad, N.S. Elazab, M. Osman, J. Phys. Soc. Jpn. **82**, 044004 (2013)
36. M. Tantawy, H.I. Abdel-Gawad, Eur. Phys. J. Plus. **137**, 1001 (2022)
37. H.I. Abdel-Gawad, M. Tantawy, A.M. Abdelwahab, Alex. Eng. J. **61**, 11225 (2022)